2014 American Control Conference (ACC)
June 4-6, 2014. Portland, Oregon, USA

Bearing-Compass Formation Control: A Human-Swarm Interaction Perspective

Eric Schoof, Airlie Chapman, and Mehran Mesbahi

***Abstract*—The paper considers the distributed formation control problem given bearing-only sensing of nearby agents with respect to a global vector frame, provided by a compass. We propose a bearing-compass control law and prove its convergence to a formation that is unique up to translation and scaling. We present results that describe the formation's evolution in terms useful to a human operator, focusing on scale, translation and rotation of the formation. The results are supported with a number of illustrative examples.**

***Index Terms*—Distributed Control; Human-Swarm Interaction; Bearing-Only Control**

I. Introduction

Formation control is an important problem in robotics. Significant of late is the problem's formulation from a distributed point-of-view, where an individual robotic agent only uses local information for its operation [1], [2]. By restricting the scope of an individual agent, the system as a whole becomes more robust to agent failure and scalable to larger numbers of agents. A common strategy employed in the literature is to generate an agent control law that relies on information obtained about other nearby agents or landmarks. One such approach uses relative bearing information and steers the agent perpendicular to these unit bearing vectors [3].

There are many approaches to distributed formation control, characterized by the states an agent can observe of its neighbors. One approach requires knowledge of the relative position of neighboring agents, either in Cartesian or polar coordinates [2]. This method is simple to implement, but requires more information than other methods. Another common approach requires knowledge of the relative distance of neighboring agents [2], [4]. This information can be obtained for example by the strength of the received wireless communication signals. The method used in this work requires knowledge of the relative bearing of neighboring agents for example from a monocular camera [5]. A mix of range and bearing information can also be used, for example when a subset of agents has the full relative position of a subset of neighbors [6], or when the distance between agents can be estimated using bearing measurements [7].

There are many works in the literature that use a bearing-only approach to formation control [8], [9], [10], [11], [12]. We complement these works by further incorporating a single additional sensor, a compass, to localize the rotation. This allows a human operator to provide global commands to the swarm without relying on external infrastructure, like GPS. Several results regarding the behavior of the control law and its stability are presented. In particular, we examine properties that would be of interest to a human operator.

Our contribution lies in the analysis of the bearing-only control problem from the perspective of a human operator. Being able to rotate, scale, and translate a formation using high-level commands is appealing since they are *intuitive* for a human operator to execute. In this paper, we show scale and centroid invariance and formation convergence with unforced dynamics for the proposed control laws. We also examine how the agents translate and scale in the presence of arbitrary additive control signals, focusing on the effects from one or two agents. Finally, we examine the behavior of the system when a single command to rotate or translate is broadcast to all agents.

The structure of the paper is as follows. In §II, we present background and notation used throughout this paper. §III contains the bearing-compass model formulation. In §IV and §V, we discuss properties relating to the unforced and forced dynamics, respectively. Finally, we present some concluding remarks in §VI.

II. Background

In this section, we provide a brief background on the notation that is used in this paper. We define the vector $\mathbf{1}_n$ as the length n vector of all ones, e_i as the vector with ith element 1, and all other elements 0, and $e_{ij} = e_j - e_i$. The matrix I_n, or I, denotes the $n \times n$ identity matrix. The notation $\|v\|$ refers to the 2-norm, or magnitude, of v. The normalized vector of v is denoted as $\hat{v} = \frac{v}{\|v\|}$. The Kronecker product of matrices A and B is denoted as $A \otimes B$. Given vectors $p, q \in \mathbb{R}^2$, the perpendicular of p is $p^\perp = R_{90} p$, where $R_{90} = \begin{bmatrix} e_2 & -e_1 \end{bmatrix} \in \mathbb{R}^{2\times 2}$, exhibiting properties $(-p)^\perp = -(p)^\perp$, $p^T q^\perp = -q^T p^\perp$ and $p^T p^\perp = 0$.

Agent positions in 2-D space at time t are represented by the vector $r(t) = \begin{bmatrix} r_1(t)^T & r_2(t)^T & \cdots & r_n(t)^T \end{bmatrix}^T$, where $r_i(t) = \begin{bmatrix} x_i(t) & y_i(t) \end{bmatrix}^T$ and agent i is at position $(x_i(t), y_i(t))$. For convenience we refer to the initial condition $r(0)$ as r_0. An undirected graph $\mathcal{G} = (V, E)$ is characterized by nodes V and edges $(i, j) \in E$, $i, j \in V$. The pair $(r, \mathcal{G})$ represents a set of agents that can communicate or observe each other over the edge set in $\mathcal{G}$, with $n = |V|$ total agents having two-dimensional positions $r \in \mathbb{R}^{2n\times 1}$ and $m = |E|$ unweighted edges. We denote the vector from agent

This research of the authors was supported by AFOSR grant FA9550-12-1-0203. The authors are with the Department of Aeronautics and Astronautics, University of Washington, WA 98105. Emails: {eschoof, airliec, mesbahi}@uw.edu.

i to agent j as $r_{ij} = r_j - r_i$. We define the set of neighbors of agent i as $j \in \mathcal{N}(i)$ if $(i,j) \in E$, where $\mathcal{N}(i)$ is called the *neighborhood* of i. The Laplacian matrix of $\mathcal{G}$ is defined as $L(\mathcal{G}) = \sum_{(i,j)\in E} e_{ij} e_{ij}^T$. If $\mathcal{G}$ is connected then $L(\mathcal{G})$ is a rank $n-1$ positive semidefinite matrix with $L(\mathcal{G})\mathbf{1} = 0$ and second smallest eigenvalue $\lambda_2(\mathcal{G}) > 0$ [2].

Two types of stability considered in this paper are almost global exponential stability and ultimately bounded stability. An equilibrium of $\dot{x} = f(x)$ having *almost global exponential stability* means that the solution converges exponentially to the equilibrium for every initial condition contained in an open and dense set whose complement is a set of Lebesgue measure zero. Consequently, the domain of attraction of the equilibrium is the whole space $r \in \mathbb{R}^n$, excluding a closed set of Lebesgue measure zero. The solutions of $\dot{x} = f(x)$ are *ultimately bounded* with ultimate bound b if there exists a b and c such that for every $0 < a < c$, there exists a $T = T(a,b) > 0$ such that $\|x(0)\| \le a \implies \|x(t)\| \le b$, for all $t \ge T$.

III. Model

We assume that there is a collection of agents each equipped with a compass and a sensor which can measure bearing to nearby agents, as defined by the edges in $\mathcal{G}$. Further, since $\mathcal{G}$ is undirected, it is assumed that if an agent i can "see" agent j, that agent j can also "see" agent i.

The 2-D formation we desire is defined by the bearing of each agent i relative to a global reference vector measured from its neighbors $\mathcal{N}(i)$. An example of such a global reference vector is north measured using a compass, while the relative bearings can be measured using a bearing sensor such as a monocular camera. Consequently, there are $2m$ bearing constraints of the form $\hat{f}_{ij} = \begin{bmatrix} \cos\theta_{ij} & \sin\theta_{ij} \end{bmatrix}^T$ for neighboring agents i and j where θ_{ij} is the desired bearing of j from i, depicted in Figure 1a. We denote the set of desired unit vectors defined over $\mathcal{G}$, which can be time varying, as $\Theta(\mathcal{G}, t) := \{\hat{f}_{ij}(t)\}$. If the underlying graph is apparent then we refer to the set simply as $\Theta(t)$.

To achieve the bearing constraints $\Theta(t)$, we use a particle model for the dynamics,

$$\begin{aligned} \dot{r}_i &= u_i(\Theta(t)) + \tilde{u}_i \\ u_i(\Theta(t)) &= \sum_{j\in\mathcal{N}(i)} \left(\hat{r}_{ij}^T \hat{f}_{ij}^{\perp}\right) \hat{r}_{ij}^{\perp}, \end{aligned} \qquad (1)$$

where $\hat{f}_{ij} \in \Theta(t)$ and $\tilde{u}_i$ is an external additive control input on agent i. When $\Theta(t)$ is constant for all t and apparent from the context, then we refer to $u_i(\Theta(t))$ as simply u_i. Given a vehicle not represented by a particle model, a more complicated control law can generally be used to track this *virtual particle* [4]. It is worth mentioning that $\|u_i\| \le |\mathcal{N}(i)|$, which is finite if the number of agents is finite. We can subsequently bound the control required of an individual agent by limiting the number of neighbors it can observe.

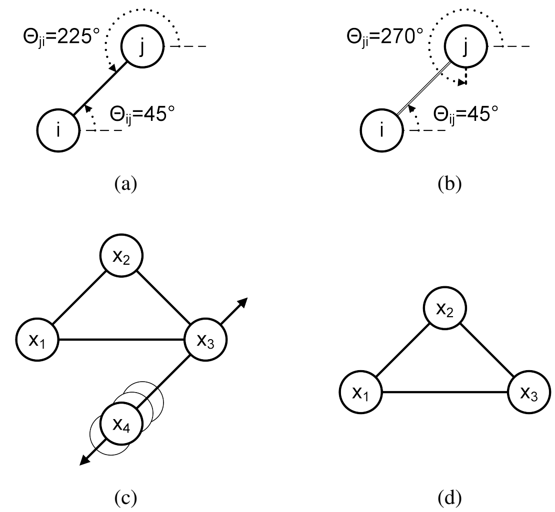

Figure 1: Bearing constraints which are a) desired (and realizable) and b) non-realizable. Formations which correspond to c) a realizable bearing, but not a parallel rigid, set and d) a parallel rigid set.

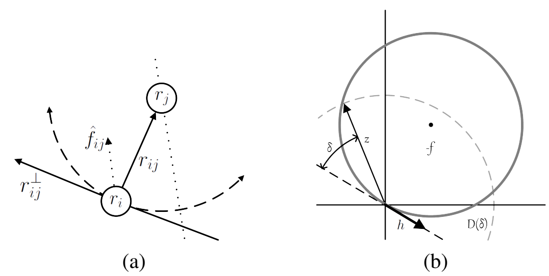

Figure 2: a) Model vector definitions. b) Geometry pertaining to Theorem 3.

For convenience we write the unforced control u_i as $u_i = \sum_{j\in\mathcal{N}(i)} u_{ij}$, where $u_{ij} = \|r_{ij}\|^{-2}\left(r_{ij}^T \hat{f}_{ij}^{\perp}\right) r_{ij}^{\perp}$ which corresponds to the contribution of agent j on the unforced dynamics of agent i. We note that $u_{ij} = -u_{ji}$, and figure 2a denotes the components of u_{ij}.

Before proceeding we briefly mention the required conditions on Θ to achieve a realizable 2-D formation that is also rigid, i.e., unique up to scaling and translation. There are many works in the literature regarding so-called formation rigidity [8], [11], [13], [14]. Consider the set

$$\begin{aligned} \chi(\Theta) &= \Big\{ \begin{bmatrix} r_1^T & r_2^T & \cdots & r_n^T \end{bmatrix}^T \in \mathbb{R}^{2n} \\ &\qquad : \hat{r}_{ij}^T \hat{f}_{ij}^{\perp} = 0 \text{ for all } \hat{f}_{ij} \in \Theta \Big\} \end{aligned}$$

composed of all 2-D n-agent positions that satisfy Θ. If $\chi(\Theta)$ is non-empty then Θ is referred to as a *realizable bearing* set [8]. Examples of a realizable and non-realizable bearing set can be seen in Figure 1b. Further, if every pair of position vectors in a realizable bearing set $\chi(\Theta)$ is equivalent to every other up to 2-D scaling and translation then Θ is called a *parallel rigid* set [8]. Figures 1c and 1d provide examples of non-parallel-rigid and parallel-rigid sets. A linear algebra test for parallel rigidity using the rank of the bearing-constrained rigidity matrix, as well as a graph theoretic test, has been formulated by Bishop *et al.* [8]. Henceforth, we shall consider only parallel rigid sets Θ.

IV. Unforced Properties

The following section explores some of the characteristics of the proposed dynamics (1). Important to human-swarm interaction is that the unforced dynamics should perform in a "predictable" fashion. One example of this is the maintenance of scale and centroid through transient dynamics. These are the first features that we explore. The second feature we investigate is the efficient convergence to a feasible formation.

Invariant Properties: Key to understanding the nuances of the dynamics is the examination of underlying invariant properties. The following two propositions shows the dynamics preserve both the centroid $C(r) = \frac{1}{n}\sum_{i\in V} r_i$ and "scale" of the dynamics defined as $S(r) = \sum_{i\in V} \|r_i - C(r)\|^2$.

Proposition 1. *Under the unforced dynamics (1), the centroid of the formation $C(r)$ is constant.*

Proof: Examining the time derivative of the centroid with $\tilde{u}_i = 0$ for all $i \in V$, and writing the dynamics in terms of the edges, $\frac{\partial C(r)}{\partial t} = \frac{1}{n}\sum_{i\in V}\dot{r}_i = \frac{1}{n}\sum_{i\in V}\sum_{j\in\mathcal{N}(i)} u_{ij} = \frac{1}{n}\sum_{(i,j)\in E}(u_{ij} + u_{ji}) = 0$. ∎

Proposition 2. *Under the unforced dynamics (1), the scale $S(r)$ is constant.*

Proof: Without loss of generality, assume $C(r)$ is initially at the origin. From Proposition 1, $C(r)$ is static. Examining the time derivative of the scale $S(r)$ with $\tilde{u}_i = 0$ for all $i \in V$,

$$\begin{aligned}
\frac{1}{2}\frac{\partial}{\partial t}S(r) &= r^T\dot{r} = \sum_{i\in V} r_i^T u_i = \sum_{i\in V} r_i^T \sum_{j\in\mathcal{N}(i)} u_{ij} \\
&= \sum_{(i,j)\in E} r_i^T u_{ij} + r_j^T u_{ji} = -\sum_{(i,j)\in E} r_{ij}^T u_{ij} \\
&= -\sum_{(i,j)\in E} r_{ij}^T \frac{1}{\|r_{ij}\|^2}\left(r_{ij}^T \hat{f}_{ij}^{\perp}\right) r_{ij}^{\perp} \\
&= -\sum_{(i,j)\in E} \frac{r_{ij}^T \hat{f}_{ij}^{\perp}}{\|r_{ij}\|^2} r_{ij}^T r_{ij}^{\perp} = 0.
\end{aligned}$$ ∎

Figures 3 and 4 provide examples of the conservation of $C(r)$ and $S(r)$ for varying bearing constraint sets Θ and initial conditions.

Lyapunov Stability : We proceed to show the convergence of the dynamics to a feasible formation $r \in \chi(\Theta)$. More precisely, the following result details almost global convergence to the set of stable equilibrium $\chi_s(\Theta) = \left\{r \in \chi(\Theta) : \hat{r}_{ij}^T \hat{f}_{ij} = 1 \text{ for all } \hat{f}_{ij} \in \Theta\right\}$, i.e., the feasible formations in which all r_{ij}'s are parallel to f_{ij}. The unstable equilibrium are composed of those feasible formations anti-parallel to $\chi_s(\Theta)$, namely the equilibrium set $\chi_u(\Theta) = \chi(\Theta) \setminus \chi_s(\Theta)$. To aid the analysis, we refer to the unique

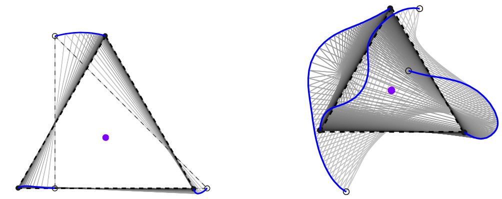
(a) (b)

Figure 3: Convergence to an equilateral triangle from a) a right triangle and b) random initial conditions. Initial and final positions are marked with open and closed circles, respectively, and the centroid by a larger solid circle. The bearing constraint formation is marked with dashed lines.

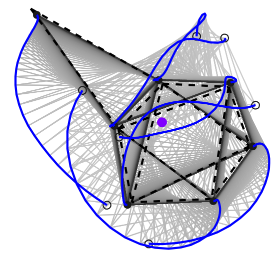

Figure 4: Random initial position on 7 agents, converging to an asymmetric formation.

stable equilibrium that the formation almost always acquires as $\xi(r, \Theta) = \{f \in \chi_s(\Theta) : C(r) = C(f),\, S(r) = S(f)\}$.

Theorem 3. *Under the dynamics (1), $r(t)$ will converge to $\chi(\Theta)$. Specifically given the initial position r_0, the equilibrium $\xi(r_0, \Theta)$ is almost globally exponential stable. Further, the rate of convergence is $\frac{1}{2m\sqrt{S(r_0)}}\lambda_2(\mathcal{G})^2\cos^2\delta$ for $r_0 \in D_r(\delta) := \{r \in \mathbb{R}^n \,|\, \|r - \xi(r,\Theta)\| \le 2\|r\|\sin\delta\}$ and $\delta \in [0, \frac{\pi}{2})$.*

Proof: Without loss of generality, let the centroid of r_0 be the origin. Let $f = \xi(r_0, \Theta)$. Consequently, $\|r_0\| = \|f\|$ and $C(f) = 0$. Applying the change of variable $z = r - f$ as $r_{ij} = z_{ij} + f_{ij}$ then for each $i \in V$,

$$\begin{aligned}
\dot{z}_i &= \sum_{j\in\mathcal{N}(i)} \hat{r}_{ij}^T \hat{f}_{ij}^{\perp} \hat{r}_{ij}^{\perp} \\
&= \sum_{j\in\mathcal{N}(i)} \frac{1}{\|z_{ij} + f_{ij}\|^2}\left(z_{ij} + f_{ij}\right)^T \hat{f}_{ij}^{\perp}\left(z_{ij} + f_{ij}\right)^{\perp} \\
&= \sum_{j\in\mathcal{N}(i)} \frac{z_{ij}^T \hat{f}_{ij}^{\perp}}{\|z_{ij} + f_{ij}\|^2}\left(z_{ij} + f_{ij}\right)^{\perp} := g_i(z, f). \qquad (2)
\end{aligned}$$

Consider the Lyapunov function $V(z) = \frac{1}{2}z^T z$ with time derivative

$$\begin{aligned}
\dot{V}(z) &= z^T\dot{z} = \sum_{i\in V} z_i^T g_i(z, f) \\
&= \sum_{(i,j)\in E} \frac{-z_{ij}^T z_{ij}^T \hat{f}_{ij}^{\perp}}{\|z_{ij} + f_{ij}\|^2}\left(z_{ij} + f_{ij}\right)^{\perp} \\
&= -\sum_{(i,j)\in E} \frac{z_{ij}^T \hat{f}_{ij}^{\perp}}{\|z_{ij} + f_{ij}\|^2}\left(z_{ij}^T z_{ij}^{\perp} + z_{ij}^T f_{ij}^{\perp}\right)
\end{aligned}$$

$$= -\sum_{(i,j)\in E} \frac{\left(z_{ij}^T f_{ij}^{\perp}\right)^2}{\|f_{ij}\| \|z_{ij} + f_{ij}\|^2}.$$

As $\dot{V}(z) \le 0$ and $\dot{V}(z) = 0$ if and only if $z \in \chi$ then $r \in \chi$ and $r(t)$ converges to χ.

We proceed to establish almost exponential stability. Note that $4\|f\|^3 \ge \max\|f_{ij}\|\left(\max\|z_{ij}\| + \max\|f_{ij}\|\right)^2 \ge \|f_{ij}\| \|z_{ij} + f_{ij}\|^2$ for all $(i,j) \in E$, $(e_{ij} \otimes I_2)^T z = z_{ij}$, and $(e_{ij} \otimes R_{90})^T f = f_{ij}^{\perp}$. Then

$$\begin{aligned}
\dot{V}(z) &\le \frac{-1}{4\|f\|^3} \sum_{(i,j)\in E} \left(z^T (e_{ij} \otimes I_2)(e_{ij} \otimes R_{90})^T f^{\perp}\right)^2 \\
&= \frac{-1}{4\|f\|^3} \sum_{(i,j)\in E} \left(z^T \left(e_{ij} e_{ij}^T \otimes R_{90}^T\right) f\right)^2 .
\end{aligned}$$

Applying the fact that $\sum_{i=1}^m q_i^2 \ge \frac{1}{m}\left(\sum_{i=1}^m q_i\right)^2$ for $q_i \in \mathbb{R}$ for all i then

$$\begin{aligned}
\dot{V}(z) &\le \frac{-1}{4\|f\|^3 m} \Big(\sum_{(i,j)\in E} z^T \left(e_{ij} e_{ij}^T \otimes R_{90}^T\right) f\Big)^2 \\
&= \frac{-1}{4\|f\|^3 m} \Big(z^T \sum_{(i,j)\in E} \left(e_{ij} e_{ij}^T \otimes R_{90}^T\right) f\Big)^2 \\
&= \frac{-1}{4\|f\|^3 m} \left(z^T \left(L(\mathcal{G}) \otimes R_{90}^T\right) f\right)^2 \\
&= \frac{-1}{4\|f\|^3 m} \left(z^T h\right)^2 ,
\end{aligned}$$

where $h := \left(L(\mathcal{G}) \otimes R_{90}^T\right) f$.

From scale invariance (Proposition 2), $\|f\| = \|r\| = \|z + f\|$, i.e., z lies on a sphere about $-f$ of radius f. Since z lies on this sphere, $z^T h = 0$ at only two points; when $z = 0$ and $z = -2f$, i.e., the end points of a diameter chord of the sphere touching the origin. Consequently, the vector h is tangent to the sphere and so $\left|z^T h\right| = \|z\| \|h\| \cos\delta$ where $\delta \in \left[0, \frac{\pi}{2}\right]$ is the angle between z and the tangent line aligned with h, and as z is on a sphere then $\|z\| = 2\|f\| \sin\delta$. Figure 2b depicts this geometry.

For $z \in D(\delta) = \{z \in \mathbb{R}^n | \|z\| \le 2\|f\| \sin\delta\}$ where $\delta \in [0, \frac{\pi}{2})$, then $r \in D_r(\delta)$ and $\left(z^T h\right)^2 \ge \|z\|^2 \|h\|^2 \cos^2\delta$ for all $z \in D$. Hence, for $z \in D(\delta)$,

$$\begin{aligned}
\dot{V}(z) &\le \Big(\frac{-1}{4\|f\|^3 m} \|h\|^2 \cos^2\delta\Big) \|z\|^2 \\
&\le \Big(\frac{-1}{4\|f\|^3 m} \|h\|^2 \cos^2\delta\Big) V(z).
\end{aligned}$$

As the centroid of f is at the origin then $(\mathbf{1}_n \otimes I_2)^T f = 0$ and so f has no component aligned with the two zero eigenvalues of $L(\mathcal{G}) \otimes R_{90}^T$, thus $\|h\| \ge \lambda_2(\mathcal{G}) \|f\|$.[1] Therefore,

$$\begin{aligned}
\dot{V}(z) &\le \Big(\frac{-1}{4\|f\|^3 m} \lambda_2(\mathcal{G})^2 \|f\|^2 \cos^2\delta\Big) \|z\|^2 \\
&= \Big(\frac{-1}{4m\|f\|} \lambda_2(\mathcal{G})^2 \cos^2\delta\Big) \|z\|^2 \\
&:= -c_3 \|z\|^2 = -2c_3 V(z). \qquad (3)
\end{aligned}$$

[1]A necessary condition for the set Θ to be parallel rigid is that $\mathcal{G}$ is connected and as such $\lambda_2(\mathcal{G}) > 0$ [8].

Therefore, the dynamics converges exponentially to $z = 0$ in the domain $z \in D(\delta)$ at the rate $2c_3$. Further, noting that the dynamics converges globally to $z = 0$, corresponding to $r = f \in \chi_s(\Theta)$, except at $z = -2f$ (an unstable equilibrium), corresponding to $r = -f \in \chi_u(\Theta)$, then the dynamics will converge almost globally. Applying the fact that $\|f\| = \|r_0\| = \sqrt{S(r_0)}$ as $C(r_0) = 0$, the result follows. ■

The convergence rate in Theorem 3 highlights initial condition and graph properties that promote the model's stability performance. The equilibrium will take longer to acquire for initial conditions with a large scale. This is a product of the previously mentioned limited-control authority of each agent i with bounded control of $\mathcal{N}(i)$. The error correction component of the control law stems from the alignment of $r(t)$ with the formation f represented by the gain $\hat{r}_{ij}^T \hat{f}_{ij}^{\perp}$. For large misalignments with r_{ij}'s close to being anti-parallel with $\hat{f}_{ij}$, this term will be small. The term $\cos^2\delta$ encapsulates the effect of this on the convergence, with $\cos^2\delta \to 0$ as $\delta \to \frac{\pi}{2}$ and so slowing convergence.

The eigenvalue $\lambda_2(\mathcal{G})$ is a well known measure of network connectivity [2], and so (on the same number of edges) the model will converge more rapidly with increased connectivity of the underlying graph. The role of $\frac{\lambda_2(\mathcal{G})^2}{m}$ can be applied to the selection of performant network topologies. Suitable candidates include those graphs where $\lambda_2(\mathcal{G})$ scales well with the number of edges m, such as random regular graphs and expander graphs [15]. Increasing $\lambda_2(\mathcal{G})$ also provides an impetus for adding more edges than required for a minimally rigid formation [8].

Figure 3 demonstrates the effect of the initial condition on the formation with a smaller δ in (a) converging faster than the larger δ in (b). The less favorable topology in Figure 4 with small $\frac{\lambda_2(\mathcal{G})^2}{m}$ compared to Figure 3 results in a slower convergence, demonstrating the importance of graph structure on the rate of convergence.

V. Forced Properties

Now that we have studied how the unforced system behaves, a natural extension is to examine how the system responds to an external control added to one or more agents. Specifically, we consider nonzero additive $\tilde{u}$'s for a subset of agents and/or a time-varying $\Theta(t)$, appearing in dynamics (1). We examine the effect of control from; an arbitrary agent set with differing control inputs, dubbed non-broadcast control and all agents applying a common control, dubbed broadcast control. Motivated by *intuitive* human-swarm interaction with the formation dynamics, we focus on control strategies that can scale, translate and rotate the formation while preferably maintaining other features of the formation.

Additive Control: We first consider the additive control via the $\tilde{u}_i$ terms. To realize this type of control in a human-swarm scenario would require a non-broadcast control signal to be sent to each agent with $\tilde{u}_i \neq 0$. The following proposition examines the effects of additive control on the centroid and scale under the dynamics (1).

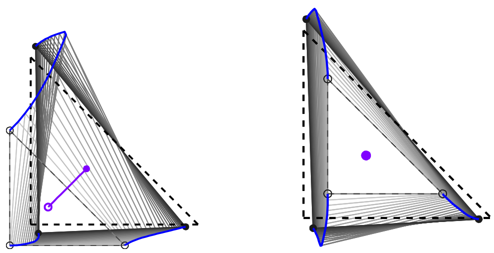

Figure 5: a) Control applied to top agent, resulting in a scale and a translation. b) Top and bottom-left agents apply a control to move away from one another, resulting in a pure scale amplification while maintaining the centroid.

Proposition 4. *Under non-zero additive control for the dynamics (1),* $\frac{\partial C(r)}{\partial t} = \frac{1}{n}\sum_{i\in V}\tilde{u}_i$ *and* $\frac{\partial S(r)}{\partial t} = 2\sum_{i\in V}(r_i - C(r))^T(\tilde{u}_i - \frac{1}{n}\sum_{j\in V}\tilde{u}_j)$*.*

Proof: Applying the invariant properties from Propositions 1 and 2,

$$\frac{\partial C(r)}{\partial t} = \frac{1}{n}\sum_{i\in V}\dot{r}_i = \frac{1}{n}\sum_{i\in V}(u_i + \tilde{u}_i) = \frac{1}{n}\sum_{i\in V}\tilde{u}_i$$

and

$$\begin{aligned}\frac{1}{2}\frac{\partial S(r)}{\partial t} &= \sum_{i\in V}(r_i - C(r))^T(\dot{r}_i - \dot{C}(r))\\ &= \sum_{i\in V}(r_i - C(r))^T(u_i + \tilde{u}_i - \frac{1}{n}\sum_{j\in V}\tilde{u}_j\\ &= \sum_{i\in V}(r_i - C(r))^T(\tilde{u}_i - \frac{1}{n}\sum_{j\in V}\tilde{u}_j).\end{aligned}$$ ■

A consequence of this result is that if a single agent, say agent i, applies a non-zero external control input, then the centroid will always shift in the direction of the applied control, namely $\frac{\partial C(r)}{\partial t} = \frac{1}{n}\tilde{u}_i$, and so $C(r) = \frac{1}{n}\int_0^t \tilde{u}_i + C(r_0)$. Further, as $\frac{\partial S}{\partial t} = 2(r_i - C(r))^T\tilde{u}_i$, changes in the centroid are coupled to changes in scale. In fact, movement away from the centroid will expand the formation while movement towards will contract it. Figure 5a provides an example of a constant control applied to a single agent demonstrating the translation and scale of the formation.

Another result following from Proposition 4 is that control of two agents can achieve scaling without translation of the formation. This scaling, unlike for the single agent case, can be achieved without knowledge of the direction of the centroid. This observation is summarized in the following corollary.

Corollary 5. *If two agents, not necessarily adjacent in $\mathcal{G}$, apply equal magnitude controls along the vector between them but in opposite directions, the centroid remains stationary while the scale $S(r)$ decreases when the agents move towards one another, and increases otherwise.*

Proof: Consider two agents i and j having a forced control $\tilde{u}_i = -\tilde{u}_j = -u$. The change in the centroid from Proposition 4 is $\frac{\partial C(r)}{\partial t} = \frac{1}{n}(\tilde{u}_i + \tilde{u}_j) = \frac{1}{n}(-u+u) = 0$. Without loss of generality, assume that the centroid is at the origin. The change in the scale from Proposition 4 is

$$\begin{aligned}\frac{1}{2}\frac{\partial S}{\partial t} &= \sum_{i\in V} r_i^T(\tilde{u}_i - \frac{1}{n}\sum_{j\in V}\tilde{u}_j)\\ &= \left(r_i^T\tilde{u}_i + r_j^T\tilde{u}_j\right) = \left(-r_i^T u + r_j^T u\right)\\ &= (r_j - r_i)^T u = r_{ij}^T u.\end{aligned}$$

Since u is parallel to r_{ij}, then $r_{ij}^T u = -\|r_{ij}\|\,\|u\|$ if the agents move towards one another and $r_{ij}^T u = \|r_{ij}\|\,\|u\|$ if they move apart. Consequently, $\frac{\partial S}{\partial t} = \pm 2\|r_{ij}\|\,\|u\|$, i.e., the dynamics experience a pure scaling proportional to the magnitude of the forced control input and the distance between agents applying the control. ■

An example of Corollary 5 can be seen in Figure 5b, whereby the formation is scaled while the centroid remains stationary.

To complement Corollary 5 we examine a scenario whereby pure translation without scaling can occur. This can be achieved using a broadcast control approach where all agents apply the same control magnitude and direction, i.e., a common additive $\bar{u}$. In practice, broadcast communication scales well with the size of the network since no agent-specific communication is required.

Corollary 6. *If all agents $i \in V$ have the same external control $\tilde{u}_i = \bar{u}$, then the centroid $C(r)$ moves as $\bar{u}$, without scaling.*

Proof: Follows directly from Proposition 4. ■

Rotation Control: We examine a non-additive type of broadcast control, one that dynamically rotates the unit vectors in Θ at a constant rate. We consider the time varying bearing set $\Theta(t) = \{\hat{f}_{ij}(t)\}$, with $\hat{f}_{ij}(t) = R(\theta(t))\hat{f}_{ij}$ for all $\hat{f}_{ij} \in \Theta$, $R(\theta) = \begin{bmatrix}\cos\theta & -\sin\theta\\ \sin\theta & \cos\theta\end{bmatrix}$ is the rotation matrix, and $\dot{\theta} = \omega \in \mathbb{R}$ is constant. This control law can be realized by broadcasting to all agents simultaneously the value $\dot{\theta}$. The dynamics becomes

$$\dot{r} = \sum_{j\in\mathcal{N}(i)}\left(\hat{r}_{ij}^T\hat{f}_{ij}^{\perp}(t)\right)\hat{r}_{ij}^{\perp}. \quad (4)$$

The equilibrium trajectory $f(t)$ of (4) is a rotation of the formation $f = \xi(r_0, \Theta)$ about its centroid, i.e., $f(t) = (I_n \otimes R(\theta(t)))(f - C(f))$. It is straight forward that $C(r)$ and $S(r)$ will be constant under this type of control. The following theorem states that the trajectory $f(t)$ will ultimately be achieved up to some bound b.

Theorem 7. *The equilibrium trajectory of (4) is bounded for all $t \geq 0$ and ultimately bounded by $b = \frac{4mS(r_0)\dot{\theta}}{\alpha(\lambda_2(\mathcal{G})^2\cos^2\delta)}$ for $r_0 \in D_r(\delta)$ and $\delta \in [0, \frac{\pi}{2})$, defined in Theorem 3, and where $\alpha \in (0,1)$ is an arbitrary constant.*

Proof: For the rotating case dynamics (4), for a *frozen* θ [16] the frozen equilibrium point is $r = (I_n \otimes R(\theta))f := f_\theta$. The frozen θ, under the change of variable $z = x - f_\theta$, has dynamics $\dot{z}_i = g_i(z, f_\theta)$, where $g_i(\cdot)$ is defined in (2), and analyzed in Theorem 3. The non-frozen rotating system consequently has dynamics, for each $i \in V$,

$$\dot{z}_i = g_i(z, f_\theta) - \frac{\partial f_\theta}{\partial \theta}\dot{\theta}. \tag{5}$$

We proceed to analyze this system as a slow varying system drawing upon the comparison lemma [16] to show ultimate boundedness. Note that $\left\|\frac{\partial f_\theta}{\partial \theta}\right\| = \|(I_n \otimes R'(\theta))\, f\| = \|f\| := L$. We have $c_1 \|z\|^2 \leq V(z) \leq c_2 \|z\|^2$, $\dot{V}(z) \leq -c_3 \|z\|^2$, $\left\|\frac{\partial V}{\partial z}\right\| = \|z\| \leq c_4 \|z\|$, and $\left\|\frac{\partial V}{\partial \theta}\right\| = 0 \leq c_5 \|z\|^2$, where c_3 is defined in (3), $c_1 = c_2 = \frac{1}{2}$, $c_4 = 1$, and $c_5 > 0$ (an arbitrary positive constant). Applying Theorem 9.3 in [16], for $\|\dot{\theta}\| \leq \epsilon$ and $z \in D(\delta)$ then the solutions of (5) are bounded for all $t \geq 0$ and ultimately bounded by

$$b = \frac{c_2 c_4 L \epsilon}{\alpha\left(c_1 c_3 - \epsilon c_2 c_5\right)} = \frac{4m\,\|f\|^2\,\dot{\theta}}{\alpha\left(\lambda_2(\mathcal{G})^2 \cos^2\delta\right)}.$$

since c_5 can be selected arbitrarily small, $\dot{\theta}$ is constant, and we can let $\epsilon = \dot{\theta}$. ∎

Not surprisingly, the bound b in Theorem 7 exhibits similar features to the convergence rate in Theorem 3. Smaller bounds are achieved with improved network connectivity, less edges, smaller scale and closer initial conditions to the equilibrium trajectory. Further, better bounds are formed with a slower rotation rate $\dot{\theta}$. These features can be observed in Figure 6, comparing (a) with larger $\frac{\lambda_2(\mathcal{G})^2}{m}$ to (b). When, the rotation rate is too high the overall formation shape can not be maintained as observed in Figure 6(d).

The additive control approach explored earlier in the section can also be combined with a rotation control. An example of this is displayed in Figure 6(c), with a rotation coupled with a pure scaling as per Corollary 5.

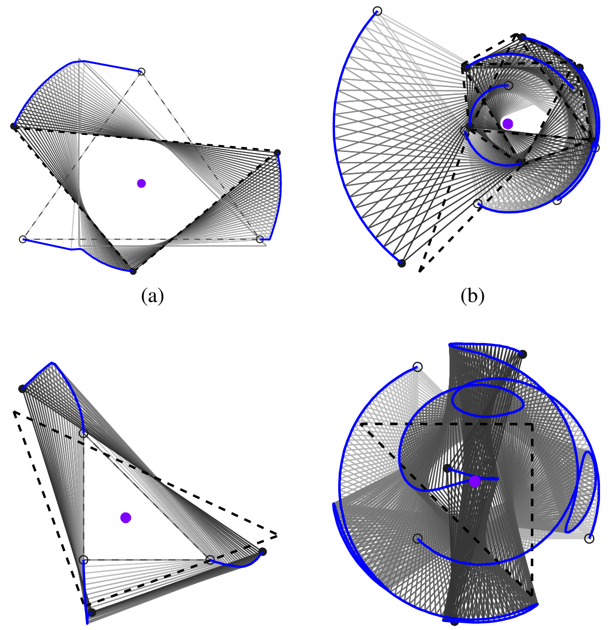
(a) (b) (c) (d)

Figure 6: Tracking a rotating formation. a) Right triangle formation. b) Asymmetric formation on 7 agents. c) Pure scale with the same additive control in Figure 5b and constant-rate rotation. d) Equilateral formation with large $\dot{\theta}$.

VI. Conclusion

In this paper, we used a common bearing-only control law applied to many agents in a decentralized network and found several properties of the system that are useful to a human operator. The invariant properties show that the centroid and scale of an arbitrary system are conserved under unforced dynamics. We have shown that we can manipulate the formation to cause rotations, scalings, and translations using one, two, or all agents. Further, we have demonstrated strong convergence guarantees for both the static and the rotating case. In the future works, we plan to extend this work into three dimensions using a unit quaternion formulation.

References

[1] R. Olfati-Saber and R. M. Murray, "Distributed cooperative control of multiple vehicle formations using structural potential functions," in *IFAC World Congress*, 2002.

[2] M. Mesbahi and M. Egerstedt, *Graph Theoretic Methods in Multiagent Networks*. Princeton, New Jersey: Princeton University Press, 2010.

[3] S. G. Loizou and V. Kumar, "Biologically inspired bearing-only navigation and tracking," in *46th IEEE Conference on Decision and Control*, 2007, pp. 1386–1391.

[4] M. Egerstedt and X. Hu, "Formation contrained multi-agent control," *IEEE Transactions on Robotics and Automation*, vol. 17, no. 6, pp. 3961–3966, 2001.

[5] A. Huster, E. Frew, and S. Rock, "Relative position estimation for AUVs by fusing bearing and inertial rate sensor measurements," in *Oceans '02 MTS/IEEE*, 2002, pp. 1863–1870.

[6] A. N. Bishop, T. H. Summers, and B. D. O. Anderson, "Control of triangle formations with a mix of angle and distance constraints," in *IEEE International Conference on Control Applications*, 2012, pp. 825–830.

[7] G. L. Mariottini, F. Morbidi, S. Member, N. V. Valk, and G. Pappas, "Vision-Based Localization for Leader-Follower Formation Control," *IEEE Transactions on Robotics*, vol. 25, no. 6, pp. 1431–1438, 2009.

[8] A. N. Bishop, I. Shames, and B. D. O. Anderson, "Stabilization of rigid formations with direction-only constraints," in *IEEE Conference on Decision and Control and European Control Conference*, 2011, pp. 746–752.

[9] A. Franchi, C. Masone, H. H. Bülthoff, and P. Robuff, "Bilateral teleoperation of multiple UAVs with decentralized bearing-only formation control," in *IEEE International Conference on Control and Automation*, 2011, pp. 2215–2222.

[10] A. N. Bishop and M. Basiri, "Bearing-only triangular formation control on the plane and the sphere," in *Mediterranean Conference on Control and Automation*, 2010, pp. 790–795.

[11] A. Franchi and P. R. Giordano, "Decentralized control of parallel rigid formations with direction constraints and bearing measurements," in *IEEE Conference on Decision and Control*, 2012, pp. 5310–5317.

[12] N. Moshtagh, N. Michael, A. Jadbabaie, and K. Daniilidis, "Vision-Based, Distributed Control Laws for Motion Coordination of Nonholonomic Robots," *IEEE Transactions on Robotics*, vol. 25, no. 4, pp. 851–860, 2009.

[13] L. Krick, M. E. Broucke, and B. A. Francis, "Stabilization of infinitesimally rigid formations of multi-robot networks," in *47th IEEE Conference on Decision and Control*, 2008, pp. 477–482.

[14] B. D. O. Anderson, C. Yu, B. Fidan, and J. M. Hendrickx, "Rigid Graph Control Autonomous Formations," *IEEE Control Systems Magazine*, no. December, pp. 48–63, Dec. 2008.

[15] B. Bollobás, *Modern Graph Theory*. New York: Springer, 1998.

[16] H. K. Khalil, *Nonlinear Systems*. Upper Saddle River: Prentice Hall, 1996.